Revealing the mechanism of Salvia miltiorrhiza Bunge and Carthamus tinctorius L herb pair in treating myocardial ischemia by combined network pharmacology and experimental verification

Shao Bing Du
Shaanxi University of Chinese Medicine
Hui Hui Zhou
Shaanxi University of Chinese Medicine
Zhi Peng Xue
Shaanxi University of Chinese Medicine
Jing Li
Shaanxi University of Chinese Medicine
Peng Fei Wang
Shaanxi University of Chinese Medicine
Xiaoping Wang (wangxiaoping323@126.com)
Shaanxi University of Chinese Medicine
Jiqing Bai
Shaanxi University of Chinese Medicine
Na Li
Shaanxi University of Chinese Medicine
Su Gao
Shaanxi University of Chinese Medicine

Research Article

Keywords: Salvia miltiorrhiza Bunge, Carthamus tinctorius L, Herb pair, Myocardial ischemia, Network pharmacology, Apoptosis

Posted Date: April 18th, 2022

DOI: https://doi.org/10.21203/rs.3.rs-1555280/v1

Abstract

The present work was aimed to gain more insight into the molecular mechanisms of Salvia miltiorrhiza Bunge and Carthamus tinctorius L herb pair (SMCTHP) in treating myocardial ischemia (MI) through network pharmacology and in vivo experiments. Firstly, various electronic databases and literatures-mining were utilized to acquire and screen out the bioactive compounds of SMCTHP and potential therapeutic targets of myocardial ischemia (MI). Subsequently, functional enrichment analysis was carried out to obtain a more radical understanding of SMCTHP against MI via the DAVID database. PPI network was established and analyzed to determine the hub targets. Finally, we used the acute myocardial ischemia (AMI) rat model to evaluate the cardioprotective effects of SMCTHP, and TUNEL assay and Western blotting analysis were used to measure the apoptotic rate and validated the hub targets and key pathways, respectively. A total of 92 bioactive compounds of SMCTHP and 245 overlapping targets between SMCTHP and MI were identified from these databases. By performing functional enrichment analysis, the anti-MI targets of SMCTHP were highly correlated with the apoptosis process, and the key functional pathways may be the PI3K/AKT and NF-κB pathways. Then, the hub targets of the PPI network contained AKT1, IL6, TNF, VEGFA, MAPK1, STAT3, RELA, MMP9, CASP3, and TLR4. In vivo experiment demonstrated that SMCTHP significantly improved myocardial ischemic injury, reduced cardiomyocyte apoptosis in ischemic rat myocardium. In addition, SMCTHP could markedly upregulate the expression of phosphorylated (p)-AKT, and obviously downregulated the expressions of TLR4 and p-NF-κBp65 in the myocardial tissue of AMI rats. This study revealed that SMCTHP may ameliorate ISO-induced myocardial ischemic injury via exhibiting the anti-apoptotic effects potentially be regulating the AKT and TLR4/NF-κB pathways.

1. Introduction

In recent years, cardiovascular diseases (CVD) have ranked first among the causes of death from diseases all over the world (Azad et al. 2020). Myocardial ischemia (MI) has become a crucial pathological process in cardiovascular diseases, commonly seen in myocardial infarction, coronary atherosclerotic heart disease and angina pectoris (Shirai. 2004; Kang et al. 2007). Currently, drugs for MI include verapamil (calcium antagonist), trimethazine (fatty acid oxidation inhibitor), isosorbide dinitrate (vasodilator), nevertheless, the clinical application of these drugs are still unsatisfactory due to adverse reactions (Liu et al. 2014). Traditional Chinese medicine (TCM) has aroused widespread interests especially in the treatment of MI due to their safety, efficacies, and low side effects (Kang. 2008; Cao et al. 2016; Li et al. 2020).

Herb pairs, the simplest form, and the centralized representation of Chinese herbal compatibility, intrinsically convey the basic idea of TCM prescriptions (Nederhoff et al. 2019). The combination of *Salvia miltiorrhiza Bunge* (SM, danshen in Chinese) and *Carthamus tinctorius L* (CT, honghua in Chinese), is a classic herb pair with removing blood stasis by promoting blood circulation and used frequently in the treatment of CVD (Orgah et al. 2020). And SM and CT interact synergistically to produce a bonding pharmacological effect greater than their individual effects in treating CVD (Yue et al. 2017). The *Salvia*

miltiorrhiza Bunge and *Carthamus tinctorius L* herb pair (SMCTHP) is the main components in multiple item preparations of treating CVD, such as *DanHongHuaYu Oral solution*, *XinNing Tablet*, *DanHong Injection* (Lyu et al. 2017). Additionally, our previous research showed that SM and CT single herb treatment effects were not significant, while the combination of these two herbs (the SM/CT ratio is 3:1) exhibited better therapeutic effects (Wang et al. 2019). Thus, the SMCTHP were investigated in the acute myocardial ischemia (AMI) rat model. Although the therapeutic effects of SMCTHP were very satisfactory in experimental research and clinical practice, its potential targets and pharmacological molecular mechanism against MI are not clear.

Network pharmacology combines the ideas of systems biology and multi-directional pharmacology. It explores the relationship between drugs and diseases from a holistic perspective and emphasizes the integration and systematicity of the interaction between drugs, targets, and diseases, and to explain the role of multiple components and multiple targets of TCM, it has been widely used in prediction of the potential active ingredients and targets of TCM and explanation of the mechanism of TCM (Luo et al. 2020). Therefore, this study revealed the potential targets and molecular mechanism of SMCTHP against MI using network pharmacology and animal experiment. The workflow of the study was shown in Fig. 1.

2. Materials And Methods

2.1. Materials and Reagents.

Isoprenaline hydrochloride (ISO) was obtained from Sigma-Aldrich (St. Louis, USA). Compound Danshen Dripping Pills were purchased from Tasly Pharmaceutical Group Co., Ltd (Tianjin, China). Total protein extraction kit, BCA protein assay kit, hypersensitive chemiluminescence reagent (ECL), anti-p-AKT, anti-AKT, anti-p-NF-κBP65, anti-NF-κBP65, anti-TLR4, anti-Cytochrome c, anti-Bax, anti-Bcl-2, anti-Caspase 3, anti-cleaved-Caspase 3, anti-Caspase 7, anti-cleaved-Caspase 7, anti-Caspase 9, anti-cleaved-Caspase 9, goat anti-rabbit IgG pre-adsorbed, anti-β-actin and anti-GAPDH were purchased from Wanleibio Co., Ltd. (Shenyang, China). Anti-Caspase 8 and anti-cleaved-Caspase 8 were purchased from Proteintech Co., Ltd. (Wuhan, China).

2.2. Network Pharmacology-Based Analysis.

2.2.1. Establishment of the Bioactive Compound Library.

Chemical compounds of SMCTHP were retrieved from Traditional Chinese Medicine Systems Pharmacology Database and Analysis Platform (TCMSP, http://ibts.hkbu.edu.hk/LSP/tcmsp.php) with the keywords "Dan Shen" and "Hong Hua", then recorded the molecule names of the compound. Next, the missed or eliminated chemical compounds are manually supplemented by literature to increase the quality of the collection.

For all compounds which were collected through the above two ways, their Chemical Abstracts Service (CAS) numbers were firstly obtained from the PubChem web platform

(http://pubchem.ncbi.nlm.nih.gov/). Then, these CAS numbers or molecule names were input into the TCMSP database separately to retrieve the ADME-related parameters of each chemical component, according to the recommendations of the TCMSP database, compounds with oral bioavailability (OB) ≥ 30% and drug likeness (DL) ≥ 0.18 were selected to construct bioactive compound library of SMCTHP (Huang et al. 2014).

2.2.2. Identification of Putative Targets for Bioactive Compound.

The putative targets of the bioactive compound in SMCTHP were respectively collected from Traditional Chinese Medicine Systems Pharmacology Database (TCMSP, http://ibts.hkbu.edu.hk/LSP/tcmsp.php) and Swiss Target Prediction (http://www.swisstargetprediction.ch/index.php). Before using of Swiss Target Prediction website, we retrieved the canonical simplified molecular input line entry specification (SMILES) and CAS numbers of all bioactive compound in the PubChem web platform. In the Swiss Target Prediction website, the canonical SMILES of bioactive compounds was uploaded with “Homo sapiens” setting, and then the compound-related targets were selected by setting the threshold value of “gene probability” as > 0.

At last, we collated and merged the relevant targets by the above two approaches. Then, we used Perl software and Uniport knowledge base to correct the name of the selected target protein to the official symbol of human gene, then eliminated duplicate targets.

2.2.3. Acquisition of Potential Targets at the Intersection of SMCTHP and MI.

With "myocardial ischemia" or "myocardial infarction" as the key word, targets related to MI were identified from the Comparative Toxicogenomics Database (CTD, http://ctdbase.org/), the DisGeNET (https://www.disgenet.org/search), the GeneCards (https://www.genecards.org/), and the National Center for Biotechnology Information database (NCBI, https://omim.org/). In the CTD database, targets with inference score greater than 100 were selected for further analysis (Li et al. 2019). In DisGeNET database, the targets satisfying ≥ 0.3 were screened out. The targets were determined from GeneCards databases with a relevance score ≥ 30 (Qu et al. 2021). In NCBI database, the targets which were belonging to Homo sapiens were selected. We summarized firstly the targets which were collected from the above four databases, then removed the duplicate values, and obtained the therapeutic targets related to MI. Finally, the overlapping targets between SMCTHP and MI were obtained and considered as the potential targets of SMCTHP in treating MI by landing on the Venny_2.1 online platform (https://bioinfogp.cnb.csic.es/tools/venny/i-ndex.html). Subsequently, the compound-target (C-T) network of SMCTHP was constructed with the Cytoscape_3.6.1 software.

2.2.4. Enrichment Analysis of GO and KEGG Pathway.

To explore the molecular mechanism of SMCTHP in the treatment of MI, GO function and KEGG pathway enrichment analysis on anti-MI targets of SMCTHP were performed in the database for Annotation,

Visualization, and Integrated Discovery (DAVID) version 6.8 (https://david.ncifcrf.gov/). Q-value < 0.01 as the screening criterion to identify the statistically significant GO terms or KEGG pathways. The bar chart of crucial GO terms and the bubble chart of crucial KEGG pathways were plotted by the Origin 2019b software. After removing cancer and other unrelated disease pathways, the GO terms and KEGG pathway of the top 15 Q-value were picked out and shown. In addition, the Kyoto Encyclopedia of Genes and Genomes (KEGG, https://www.kegg.jp/) was used to explore the interactions between top 15 significant pathways, and then the Pathway-Pathway interaction network was visualized using Cytoscape_3.6.1 software.

2.2.5. Protein-Protein Interaction Network Construction.

The STRING online website (https://string-db.org/) was applied to explore the interactions between the overlapping proteins targets of SMCTHP and MI. In this study, the species was limited to "*Homo sapiens*", with a confidence level of 0.7, and not interacting proteins were hidden. Then, a "string_interactions.tsv" file was exported and imported into the Cytoscape_3.6.1 software to visualize protein–protein interaction (PPI) network, and the topology parameters of the nodes were calculated by Network Analyzer, where the network was treated as undirected. At the same time, the CytoHubba plugin the software was utilized to screen the hub targets, and the "Degree" algorithm was selected. Densely interaction areas in PPI network were also found by means of the Molecular Complex Detection (MCODE) plugin of Cytoscape 3.6.1 software, based on the flowing default parameters of MCODE: Degree Cutoff = 2; Node S-core Cutoff = 0.2; K-Core = 2; Max. Depth = 100. Then, the significant modules of the PPI network were identified and screened. Finally, the modules generated by the pl were ranked by the size of the score, and the most significant modules were selected.

2.3. Experimental Verification.

2.3.1. Preparation of SMCTHP Extract.

SM (NO. 37172620191011YC) was collected from Heze City, Shandong Province, China. CT (NO. 65422520190906YC) was collected from Tacheng City, Xinjiang Province, China. And they were authenticated by Professor Ji-Qing Bai from Shaanxi University of Chinese Medicine, their morphological and chemical authentications were consistent with the standard of Chinese pharmacopeia 2015. These samples have been deposited in the Herbal Medicine Museum of Shaanxi University of Chinese Medicine, Xi'an, China.

Firstly, SM (900g) and CT (300g) were mixed and soaked in 50% ethanol (sample: solvent, 1:10, w/v) for 30 minutes, then warm immersed (45°C) twice for 1h of each time, filtered, filter residue was warm immersed (45°C) twice with 12000 ml distilled water for 1h of each time, filtered. Next, all the filtrates were combined and concentrated a thick paste under reduced pressure, and then freeze-dried into powder. The SMCTHP powder was dissolved in water (0.48 g/mL) for animal study.

2.3.2. Quality Control for SMCTHP.

To ensure the quality of SMCTHP, high performance liquid chromatography (HPLC) was performed to identify the composition in SMCTHP extract. The criteria for the quality of herbs in SMCTHP were in accordance with the 2020 Chinese Pharmacopeia (the information regarding reference standards was provided in Supplementary Table S1). In detail, 4 μl of SMCTHP extract (10.08 mg/ml) and different volumes of five standards (2 μl of 8.4 μg/ml danshensu, 2 μl of 6.7 μg/ml hydroxysafflor-yellow-a, 2 μl of 5.8 μg/ml rosmarinic acid, 5 μl of 3.6 μg/ml lithospermic acid, 2 μl of 31.5 μg/ml salvianolic acid b) were respectively injected into the HPLC system (Thermo Fisher Scientific, USA). The separation was performed on the Thermo Hypersil GOLD C18 (250 mm×4.6mm, 5 μm) column with acetonitrile (A)–0.2% phosphoric acid aqueous solution (B) (0–15, maintained at 5% A; 15–40min, 5–10%A; 40–130min, 10–20%A; 130–150min, 20–23%A; 150–180min, 23–60%A; 180–200min, 60–100%A; 200–210min, 100%A), at flow rate of 1.0 mL/min. The column temperature was 25°C, and the detection wavelength was 288 nm.

2.3.3. Experimental Animals and Design.

40 male Sprague-Dawley (SD) rats (220–250 g), which were purchased from Sichuan Chengdu Dashuo experimental animal Co., Ltd. (SCXK (Chuan) 2020-030). Before the preparation of the AMI model, experimental rats were housed in a conditioned laboratory environment (relative humidity: 60 ± 5%, temperature: 20 ± 2°C, light: 12-hour light/dark cycle), and freely getting food and water, to adapt the laboratory conditions for a week. All animals were fasted for 12 h before the experiment and during the period of samples collection but got water.

The animals were randomly divided into six groups (n = 10 per group) in the light of their body weight: Normal group; Model group; Positive group (0.073 g/kg, 1-fold of clinical equivalent dosages); SMCTHP low-dose group (1.2 g/kg, 0.5-fold of clinical equivalent dosages); SMCTHP medium-dose group (2.4 g/kg, 1-fold of clinical equivalent dosages); SMCTHP high-dose group (4.8 g/kg, 2-fold of clinical equivalent dosages). SD rats in the Normal group, and Model group were given the same saline volume by oral gavage for consecutively 7 days. Those in the SMCTHP low-dose group, SMCTHP medium-dose and SMCTHP high-dose groups was respectively given with 1.2 g/kg/d, 2.4 g/kg/d, and 4.8 g/kg/d SMCTHP by oral gavage for 7 days. The rats in the Positive group were given 0.073 g/kg/d of Compound Danshen Dripping Pills (CDDP), which was dissolved in distilled water, by oral gavage for 7 days. Except for the Normal group, all groups were injected intraperitoneally with ISO (85 mg/kg/d) dissolved in saline on the 6th and 7th day to induce experimental myocardial ischemia (Qu et al. 2020). After 12 h following the last injection of ISO, the fresh heart tissues of sacrificial rats were removed rapidly and washed directly with cold physiological saline. One part of the heart tissues was frozen at -80 ℃ used for western blotting analysis. The other heart tissues were fixed in 10% neutral formaldehyde, embedded in paraffin wax, and stained with hematoxylin and eosin (H&E) for pathological analysis.

2.3.4. Hematoxylin-Eosin Staining.

After fixed in 10% neutral formaldehyde, the myocardium tissues of rats were washed for 4 hours with tap water and then successively dehydrated with different concentration of alcohol (75%, 85%, and 95%

ethanol, followed by anhydrous ethanol). Next, the dehydrated tissues were embedded in paraffin and cut into 5μm continuous sections and stained with H-E solution for histopathological examination (200×).

2.3.5. Serum Myocardial Enzyme Assays.

The AST and CK-MB in serum were detected by using an Olympus AU-640 automatic biochemistry analyzer (OLYMPUS OPTICAL Co., Ltd., Japan). The CTn-I in serum were determined using specific enzyme-linked immunosorbent assay (ELISA) kits obtained from Senberger Biotechnology Co., Ltd (Nanjing, China) strictly according to the regent instruction.

2.3.6. Terminal Deoxynucleotidyl Transferase dUTP Nick End Labeling Assay.

TUNEL assay was used for detection of cardiomyocyte apoptosis in rats. The detection steps were as follows:(1) The myocardium tissues were fixed in 10% neutral formaldehyde at room temperature, and then watered with flowing water for 4h, and dehydrated successively with 70% (2h), 80% (overnight), 90% (2h), anhydrous ethanol I (1h) and anhydrous ethanol II (1h). (2) The tissues were soaked in xylene for 30 minutes until the specimen is transparent and were moved into xylene + paraffin, then put into temperature box at 60 ℃ for 2 hours to allow the paraffin to permeate the tissues completely, and buried in paraffin, and cut into 5μm thin sections with a paraffin slicer (Leica, Germany). (3) The thin sections were spread out in warm water, dried in a 60 ℃ incubator for 4 hours, then placed in slicing shelves, and roasted in the oven at 60 ℃ for half an hour, then taken out and successively soaked for 30 minutes using xylene I, xylene II, anhydrous ethanol I and anhydrous II, then taken out again and successively placed in 95%, 85%, 75% and distilled water for 2 minutes, then the sections were taken out and immersed PBS for 5 minutes. It is worth noting that the residual liquid must be shaken off before soaking. (4) Tissues were permeability in 50 μl 0.1% Triton-X 100 (Beyotime, China) for 8 min at room temperature. After washed 3 times with PBS each time 5 minutes, tissues were blocked by using 50μL 3% hydrogen peroxide. After washed 3 time with PBS each time 5 minutes again, the samples were incubated with TUNEL reaction Solution (Wanleibio, China) including Enzyme solution and Label Solution at 37°C for 60 minutes. (5) The sections were rinsed in PBS and incubated with 50 μl of DAB substrate (Solarbio, China) for 10 min at room temperature, then again rinsed in PBS and further counterstained with hematoxylin (Solarbio, China). The TUNEL positive cardiomyocytes cells were stained brown. (6) These stained sections were successively dehydrated and sealed. Finally, the pathological staining results were observed under the microscope (Olumpus, Japan) at ×400 magnification. Apoptosis rate was calculated as the ratio of TUNEL positive cardiomyocytes cell to total number of cardiomyocytes cell.

2.3.7. Western Blotting.

Western blotting was a qualitative and semi-quantitative analysis method for proteins. The experimental steps were as follow: (1) The protein extraction of myocardium tissues was carried out with total protein extraction kit including lysis buffer and protease inhibitor, and then stationarily placed on ice for 5 minutes, then the lysate was centrifuged 12,000 rpm for 10 min at 4 ℃ and the supernatant was collected. (2) The protein concentrations of supernatant were calculated using the BCA protein assay kit.

According to different molecular weights of the proteins, the corresponding concentration of polyacrylamide gels was prepared. The protein of the sample was successively separated by 5% stacking polyacrylamide gel, and 10%, 15% separation polyacrylamide gels, then transferred to polyvinylidene fluoride (PVDF) membrane (Merck Millipore, USA). (3) The PVDF membranes were blocked with 5% nonfat milk powder for 1 h and incubated overnight at 4 ℃ with appropriate primary anti-bodies including that anti-p-AKT (WLP001, 1:500;), anti-AKT (WL0003b, 1:1000), anti-p-NF-κBp65 (WL02169, 1:500), anti-NF-κBp65 (WL01980, 1:500), anti-TLR4 (WL00196, 1:500), anti-Cytochrome c (WL02410, 1:500), anti-Bax (WL01637, 1:500), anti-Bcl-2 (WL01556, 1:1000), anti-Caspase 3 (WL02117, 1:500), anti-cleaved-Caspase 3 (WL02117, 1:500), anti-Caspase 7 (WL02360, 1:400), anti-cleaved-Caspase 7 (WL02360, 1:400), anti-Caspase 9 (WL03421, 1:500), anti-cleaved-Caspase 9 (WL03421, 1:500), anti-Caspase 8 (13423-1-AP, China; 1:1000) and anti-cleaved-Caspase 8 (13423-1-A, 1:1000), then sealed with a film press. (4) After that, the PVDF membranes were rinsed 4 times in TBST and were incubated with HRP-conjugated anti-rabbit IgG (WLA023, 1:5000) at 37℃ for 45 minutes. (5) Next, membranes were washed six times in TBST and were incubated with ECL system, then exposed in a darkroom. (6) Finally, films were scanned, and the optical densities of the bands were analyzed with Gel Pro-Analyzer software (Media Cybernetics, USA). GAPDH and β-actin were regarded as the internal control and the expression levels of all proteins were standardized to the internal control.

2.4. Statistics Analysis.

In this study, the experimental data were showed as mean ± standard deviation. To observe whether there is statistical significance among experimental data of multiple groups, one-way repeated-measures ANOVA followed by the Tukey's multiple comparison test were performed with Graphpad Prism 8 software. Differences with a value $P < 0.05$ was determined as statistically significant.

3. Results

3.1. HPLC Profiles.

By detecting and comparing the peak times of the test sample and standard samples, danshensu, hydroxysafflor-yellow-a, rosmarinic acid, lithospermic acid, salvianolic acid b could be identified in the SMCTHP chromatogram, and the quality standard of SMCTHP was established. The chromatogram of these seven compounds in SMCTHP powder was shown in Fig. 2, and the content of these compounds was listed in Table 1.

Table 1
Determination results of five active components in SMCTHP (mg/g).

Compounds	Content (mg/g)
danshensu	3.5737
hydroxysafflor-yellow-a	13.2530
rosmarinic acid	1.5447
lithospermic acid	3.6210
salvianolic acid b	44.3216

3.2. Network Pharmacology-Based Analysis.

3.2.1. Construction of Bioactive Compound Database.

A total of 378 chemical compounds of SMCTHP were retrieved from TCMSP and manually supplemented. The major pharmacological active compounds of SM are consisted of lipid-soluble diterpenoid compounds and hydrophilic phenolic compounds, whereas the main compounds of CT are the C-glucosylquinochalcone family of flavonoids which possess one or more glucose units. Detailed information about these compounds were provided in Supplementary Table S2.

According to the screening criteria suggested by the TCMSP database, 92 bioactive compounds were collected. Among them, 72 bioactive compounds were obtained from SM, 24 bioactive compounds from CT, and 4 overlapping compounds (SC-1 = porifera-st-5-en-3beta-ol, SC-2 = baicalin, SC-3 = luteolin and SC-4 = caffeic acid) from SM and CT.

Moreover, among compounds under these criterions, eleven compounds (salvianolic acid b, proto-catechualdehyde, danshensu, lithospermic acid, salvianolic acid a, salvianolic acid c, protocatechuic acid, hydroxysafflor-yellow-a, nicotiflorin, caffeic acid) were also considered as bioactive compounds through literature review (Shen et al. 2014; Chen et al. 2016; Hu et al. 2017; Wang et al. 2019). To understand this problem more comprehensively and objectively, we still included them in the bioactive compounds database for further analysis (Supplementary Table S3).

3.2.2. Collection of Potential Targets.

In the previous research, we have established the bioactive compound-target database of SMCTHP, and the target related to MI database. By collecting and predicting compound-target, 883 potential targets were validated from 90 active compounds, 2 compounds (SM-44 = Miltirone and CT-20 = Phytofluene) have on targets (Supplementary Table S4). 93 therapeutic targets of MI were finally collected from the GenesCards database, 274 from the DisGeNet database, 362 therapeutic targets from the CTD database, 703 from the NCBI database. After deleting the duplicate targets, 957 MI-related therapeutic targets were obtained from four databases. Then, the targets corresponding to the bioactive compounds with the MI-

related targets were intersected and thus 245 overlapping targets were generated, suggesting that these targets may be the molecular targets that mediate the anti-MI effects of SMCTHP (Fig. 3). Details of the 245 anti-MI targets were listed in Supplementary Table S5. With the support of target fishing, 207 MI-related targets were related to 71 bioactive compounds in SM. Meanwhile, 190 MI-related targets were related to 24 bioactive compounds in CT. Interestingly, 152 MI-related targets not only were associated with the bioactive compounds in SM but also with the bioactive compounds in CT, including AKT1, CASP3, CASP9, Bcl-2, CASP8, and so on.

3.2.3. The C-T Network.

Bioactive compounds and anti-MI targets of SMCTHP were imported into Cytoscape_3.6.1 software, for building the C-T visual network as shown in Fig. 4. The C-T network contained 334 nodes (89 composite nodes and 245 target nodes) and 1822 edges. In this network, the nodes represent the bioactive compounds or the therapeutic targets of MI, and edges reflected the relationship between the bioactive compounds and the corresponding therapeutic targets. The C-T network displayed those multiple targets could be acted by the same bioactive compound and multiple bioactive compounds also shared the same target, proving the multitarget treatment characteristics of SMCTHP.

3.2.4. Functional Enrichment Analysis.

To elucidate the relevant biological function and pharmacological mechanism of SMCTHP against MI, KEGG and GO enrichment analysis were implemented, respectively. Through GO enrichment, 329 process terms with q-value less than or equal to 0.01 of the 1081 process terms were identified, including 251 biological process (BP), 47 molecular function (MF) and 31 cellular components (CC) (Supplementary Table S6). As shown in Fig. 5, the leading 15 crucial enriched entries in the BP, CC, and MF terms were picked. Notably, the top 3 biological processes according to gene counts were positive regulation of transcription from RNA polymerase II promoter (GO:0045944), negative regulation of apoptotic process (GO:0043066), response to drug (GO:0042493). The enriched MF ontologies were tightly correlated with protein binding (GO:0005515), enzyme binding (GO:0019899), identical protein binding (GO:0042802), growth factor activity (GO:0008083), and so on. The plasma membrane (GO:0005886), cytosol (GO:0005829), extracellular exosome (GO:0070062) accounted for the main proportion in CC analysis.

Through KEGG pathway enrichment, 51 significant pathways ($q < 0.01$) were obtained (Supplementary Table S7). As shown in Fig. 6A, these anti-MI targets were mainly enriched in TNF signaling pathway (hsa04668), HIF-1 signaling pathway (hsa04066), PI3K/Akt signaling pathway (hsa04151), Apoptosis (hsa04668), and NF-κB signaling pathway (hsa04668). The bubble chart of KEGG pathways analysis clearly indicated that most of these pathways were enriched by multiple targets.

3.2.5. SMCTHP-MI PPI Network Analysis and Module Screening.

The 245 potential anti-MI targets were uploaded to the STRING database, for observing the relationship of these protein interactions and searching for some proteins playing an important role in the PPI network. To construct a PPI network based on high confidence, ten targets (KCNMA1, TYMP, ABCC9, SLC22A2, GRK2, CA3, FAP, PDE3A, MIF and FTO) with confidence less than 0.7 were excluded. The SMCTHP-MI PPI network consisted of 235 nodes, which interacted with 2103 edges (Fig. 7A). The size of a node is proportional to the degree value. Thicker lines indicate stronger interactions. To determine hub targets which may have a crucial role in the entire SMCTHP-MI PPI network, the Cytoscape's plugin Cytohubba was used to perform topology analysis. Topology analysis indicated that top 25 hub targets in the structural network were determined as targets for further screening, including AKT1, IL6, TNF, VEGFA, MAPK1, STAT3, JUN, CXCL8, MAPK8, MAPK3, APP, RELA, EGFR, SRC, IL1B, MMP9, MYC, PTGS2, IL10, CASP3, ALB, IL2, HSP90AA1, CCL2, and TLR4 (Fig. 7B). It can be inferred from the results that these hub targets are highly associated with other targets and may be core targets in SMCTHP against myocardial ischemia. The topology parameters of hub targets are listed in Supplementary Table S8.

KEGG pathway enrichment analysis and PPI network analysis suggested that both pathway enrichment analyses and hub targets were closely related to TNF signaling pathway, PI3K/Akt signaling pathway, Apoptosis and NF-κB signaling pathway. Interestingly, TNF, PI3K/Akt, and NF-κB signaling pathway signaling pathways mainly involve in the apoptotic process (Negoro et al. 2001; Hori et al. 2009; Luan et al. 2019). The KEGG pathway interaction network also showed that the apoptosis pathway interacted with the above three pathways (Fig. 6B). Among them, the extracellular pathway of apoptosis was mediated by the TNF receptor superfamily, while the cell hypoxia mediates the endogenous pathway (Hamacher et al. 2006). For biological process, the anti-MI targets of SMCTHP were remarkably participated in negative regulation of apoptotic process. Simultaneously, among the twenty-five hub targets, the AKT1, TLR4, and RELA (as called NF-κBp65) respectively participated in the regulation of PI3K/Akt signaling pathway and NF-κB signaling pathway, which controlled cell survival, and apoptosis (Negoro et al. 2001; Luan et al. 2019). Furthermore, the Cytochrome c, Caspase 8, Caspase 7, Caspase 9, Caspase 3, Bcl-2, Bax, TGFβ1 and mTOR are also regarded as pivotal apoptotic regulators (Ou et al. 2017; Sanches-Silva et al. 2020). Hence, we speculated that anti-apoptotic effects might be potential molecular mechanisms of SMCTHP against MI.

To further reveal the anti-apoptotic mechanisms of SMCTHP in the treatment of MI, the PPI network was divided into 14 clusters by using the MCODE plugin. As shown in Fig. 7C, the most significant modules were screened out and contained 58 targets and 681 edges. The apoptotic-related targets involved in the module were marked in red. These apoptotic-related proteins with red-labeled color were tightly correlated with PI3K/Akt pathway and NF-κB pathway (Negoro et al. 2001; Luan et al. 2019; Ou et al. 2017; Sanches-Silva et al. 2020). These findings provided the powerful support for revealing the probable anti-apoptotic mechanisms of SMCTHP against myocardial ischemia. Nevertheless, the credibility of these inferences needs to be increased by further animal experimental validation.

3.3. Experimental Verification of Results.

3.3.1. Effects of SMCTHP on the Histopathological Damages and Myocardial Specific Enzymes in Serum.

Histopathological staining supplied the definitive evidence of the anti-MI effects of SMCTHP against ISO-induced myocardial ischemia. As shown in Fig. 8A, the myocardium structure of the Normal group was intact, with an arrangement neatly of the myocardial cells, and without any necrosis and inflammatory cells. Compared with normal rats, the myocardial tissue from ISO-induced myocardial ischemia rats revealed inflammatory cell infiltration, disordered myocardial fibers arrangement, swollen and loose myocardial interstation, blood cell spillage, the consolidation and fragmentation of cardiomyocytes nucleus. SMCTHP treatment (1.2, 2.4 and 4.8 g/kg/d groups) partially attenuated these pathological changes, with the most improvement in the SMCTHP high-dose group. In addition, CDDP also could obviously improve the myocardial tissue pathological damages (Fig. 8A). As shown in Fig. 8B, serum levels of aspartate aminotransferase (AST), creatine kinase-MB (CK-MB) and cardiac troponin I (CTn I) were significantly enhanced in the Model group compared with the Normal group ($p < 0.01$). After treatment with varied SMCTHP (1.2, 2.4 and 4.8 g/kg/d) and CDDP, the levels of these myocardial specific enzymes in serum were notably decreased ($p < 0.01$).

Among the three SMCTHP groups, SMCTHP (4.8 g/kg/d) exhibited the best callback effect on these enzymes levels, the trend is consistent with HE examination results. These results indicated that SMCHTP has protective effects on myocardial ischemic injury, and the optimal dose of treatment is 4.8 g/kg/d, which was thus used for further validation of its anti-MI mechanisms.

3.3.2. Effects of SMCTHP on Cardiomyocyte Apoptosis and the Expression of Apoptosis-Related Protein.

The TUNEL assay was performed to evaluate the effect of SMCTHP on cardiomyocyte apoptosis. After TUNEL staining, the nucleus of normal cardiomyocyte cells should be stained in blue-black and the morphology of TUNEL positive cells displayed shrinkage of the cell bodies, pyknosis of the nucleus, chromatin condensation, and brownish yellow particles, showing the apoptotic characteristics. As shown in Fig. 9A, a significant increase in the number of apoptotic cell nucleus stained with brownish yellow were observed in the Model group and apoptosis rate was significantly increased compared with the Normal group ($p < 0.01$). However, it was proved that SMCTHP treatment could distinctly decrease the number of apoptotic cardiomyocytes ($p < 0.01$).

Furthermore, the protein levels of apoptosis-related proteins in rat myocardium were detected by western blotting. As Fig. 9B indicated, compared with the Normal group, a significant increase in the expression levels of Cytochrome c, Caspase 8, Caspase 7, Caspase 9, Caspase 3 and Bax in the myocardial tissue of rats ($p < 0.01$, $p < 0.05$), and a significant decrease in the expression levels of Bcl-2 ($p < 0.01$) in the myocardial tissue of rats was observed in the Model group. Compared with the Model group, the expression levels of Cytochrome c, Caspase 8, Caspase 7, Caspase 9, and Caspase 3 in the myocardial tissue of rats were significantly reduced ($p < 0.01$, $p < 0.05$), the expression level of Bcl-2 in the myocardial

tissue of rats was significantly increased in the SMCTHP group ($p < 0.05$). The Western blotting analysis results were consistent with the results of TUNEL assay. These results suggested that SMCTHP may show an anti-apoptosis effect to ameliorate the ischemic injury.

3.3.3. Effects of SMCTHP on AKT, TLR4 and NF-κB p65 Protein Levels in Ischemic Rat Myocardium.

To investigate the possible anti-apoptotic mechanism of SMCTHP in the ischemic rat myocardium, the expression levels of total AKT, total NF-κBp65, p-AKT, p-NF-κBp65, and TLR4 were detected according to network analysis results. As shown in Fig. 10 indicated, the total protein levels of AKT and NF-κBp65 in the myocardial tissue of rats had no significant difference among the four groups. Compared with the Normal group, the Model group significantly upregulated the expression of p-NF-κBp65 and TLR4 in the myocardial tissue of rats ($p < 0.01$, $p < 0.05$), and significantly downregulated the expression levels of p-AKT ($p < 0.01$) in the myocardial tissue of rats in the Model group. Compared with the Model group, the expression levels of p-NF-κBp65, and TLR4 in the myocardial tissue of rats were significantly reduced ($p < 0.01$, $p < 0.05$), the expression level of p-AKT in the myocardial tissue of rats was significantly increased in the SMCTHP group ($p < 0.01$). These results suggested that SMCTHP may inhibit cardiomyocyte apoptosis by activating the AKT pathway but suppressing the TLR4/NF-κB pathway.

4. Discussion

The AMI animal model was mainly established by open thoracotomy, closed-chest surgery, drugs, and so on. The thoracotomy has large trauma, and the survival rate of experiment animals was not ideal; The closed-chest coronary artery catheterization is usually performed by two steps: (1) The guidewire is placed in the coronary artery ahead of time after the arterial puncture; (2) the emboli is inserted into the target vessel along the guidewire through the catheter. This method has small trauma, which is conducive to the recovery of experimental animals in the later stage and the survival rate of animals is high, but it requires experimental technicians to have rich experience in cardiac catheterization experiments. Currently, drug modeling is a common approach for establishing the AMI animal model because it is relatively close to the pathological state of human angina pectoris, and it is simple to operate, and the recovery time of animals is short. The commonly used modeling drugs are pituitrin (Pit) and ISO. ISO is a strong β-receptor agonist, and its high dose can induce irreversible ischemic injury of myocardium. The ISO can be administered by two ways: intraperitoneal injection and subcutaneous injection, and the replicated acute myocardial ischemia model induced by ISO is stable (Wang et al. 2017; Fan et al. 2018; Lu et al. 2018; Chen et al. 2021). Therefore, ISO was employed to establish the AMI rat model in this study. Compound Danshen Dripping Pills, as the first formula affirmed by the US Food and Drug Administration, demonstrated an excellent effect on ischemic heart disease (Tian et al. 2005), was thus used as a positive control drug.

In the present study, the cardioprotective effect and potential molecular mechanism of SMCTHP against ISO-induced myocardial ischemic injury were investigated with the exploratory network pharmacology

analysis and related experimental verification. As a result, the major findings were divided into five parts: (1) 92 bioactive compounds and 245 anti-MI targets were identified based on electronic databases and literatures-mining, and then the compounds-target network (C-T) was established, revealing the anti-MI effect of SMCTHP is multi-component and multitarget; (2) Functional enrichment analysis with the DAVID database, and Module analysis with the Cystoscope_3.6.0 software were respectively performed, suggesting that the anti-apoptotic process may be one of the main mechanisms for SMCTHP to achieve the anti-MI effect. Meanwhile, the PI3K/AKT, NF-κB signaling pathways were regarded as the critical pathways for the anti-apoptotic action of SMCTHP; (3) PPI network analysis screened out the twenty-five hub targets, such as AKT1, IL6, TNF, VEGFA, MAPK1, STAT3, RELA, MMP9, CASP3, TLR4, and so on, indicating that these hub targets may play an essential role in the therapeutic effect of SMCTHP on MI; (4) Animal experimental results shown that all three SMCTHP groups reversed the pathological damage, decreased the biochemical markers of myocardial injury, and the optimal dosage is 4.8 g/kg/d; (5) TUNEL analysis and Western blotting analysis results suggested that SMCTHP ameliorated the myocardial ischemic injury by suppressing cardiac apoptosis via the regulation of the AKT and TLR4/NF-κB pathways.

Firstly, a total of 254 anti-MI targets of SMCTHP were determined by retrieving a series of related databases, and then the various pharmacological networks were construed and analysis. Then, GO enrichment analysis revealed that SMCTHP exhibit the anti-MI effects by involving in the multiple biological processes, including negative regulation of apoptotic process, inflammatory response, angiogenesis, and response to hypoxia. The KEGG pathway enrichment analysis revealed that the underlying biological mechanism of SMCTHP against MI was closely associated with TNF signaling pathway, HIF-1 signaling pathway, PI3K/Akt signaling pathway, Apoptosis pathway, VEGF signaling pathway and NF-κB signaling pathway, which were consistent with the reported literatures (Jayachandran et al. 2010; Ding et al. 2013; Xu et al. 2013; Ma et al. 2018; Zhu et al. 2019; Song et al. 2020). More importantly, the most meaningful module 1 was screened out with the MCODE plugin of the Cystoscope_3.6.0 software. And the targets of this module were highly concerned with apoptosis, which were labeled as the red color. The apoptosis-related protein with red-labeled color were mainly enriched in PI3K/AKT pathway, NF-κB pathway, and so on. These findings indicated that the anti-apoptotic action of SMCTHP may be an essential mechanism in the treatment of MI. Thus, this study further investigated the anti-apoptotic effects and possible mechanisms of SMCTHP on ischemic rat myocardium.

Apoptosis plays an important role in myocardial ischemia and subsequently involves in left ventricular remodeling and heart failure, which can be mediated by two main pathways: the receptor-mediated (extrinsic) and the mitochondrial (intrinsic) pathway (Yue et al. 2017; Lin et al. 2018; Wang et al. 2019; Teringova et al. 2017). It is considered that the initiation of the apoptosis process is an important factor leading to myocardial ischemic necrosis (Zhao et al. 2001). Inhibition of cardiomyocyte apoptosis protects the myocardial tissues from ischemia injury and ameliorates the cardiac function (Al-Amran et al. 2017). When the death ligand binds to its corresponding cell surface death receptor, the extrinsic pathway is initiated. Subsequently, the Caspase 8 is activated, leading to the beginning of the apoptotic cascade through processing of downstream effector caspases such as caspase 3, 7, and the pro-

apoptotic Bcl-2 family member, Bid, resulting in the cell death (Hamacher-Brady et al. 2006). Under the action of various pathophysiological factors (e.g., oxidative stress and calcium overload), the mitochondria partake in the apoptosis process (Desagher et al. 2000). Bcl-2 and Bax are a group of apoptosis-related gene proteins. Bcl-2 is a gene that inhibiting apoptosis, while Bax is a gene that promoting apoptosis. They are unified opposites and jointly determine the threshold of cell death (Misao et al. 1996). When the death signal is transmitted to the mitochondria, Bax molecule transfers from cytoplasm to mitochondrial outer membrane, resulting in the change of the molecular conformations, then promoting the opening of mitochondrial permeability transition pore (Harris et al. 2000; Uchiyama et al. 2004). After opening, Cytochrome c was released into the cytosol, in which it combines with the apoptosis protease activation factor (APAf-1) to form the apoptosome. The complex activates procaspase 9, which is triggering an enzymatic cascade, causing the cell apoptosis (Huang et al. 2016; Chimenti et al. 2018). In this study, we observed that SMCTHP could effectively reduce the cardiomyocytes apoptosis ratio and reversed ISO-induced abnormal protein expression levels of Cytochrome c, Caspase 3, Caspase 7, Caspase 8, Caspase 9, Bcl-2, and Bax, strongly suggesting that SMCTHP exhibited an anti-apoptotic effect on ischemic rat myocardium.

Based on the predictive results of network analysis, the anti-apoptotic mechanism of SMCTHP was further investigated. PPI network analysis results suggested that AKT1, NF-κBp65, and TLR4 exerted the higher degree value and belong respectively to PI3K/Akt pathway and NF-κB pathway, which are highly correlated with apoptotic process, thus their expressions were detected in vivo. PI3K/Akt signaling pathway, a classical signal transduction pathway, plays a critical role in regulating the cell growth, survival, differentiation, apoptosis (Martini et al. 2014). AKT, as the key regulatory factor, can modulates the activities of various downstream proteins such as Bcl-2 and Bax to control the cell apoptosis and proliferation (Jian et al. 2015). In addition, growing studies have demonstrated that the TLR4/NF-κB pathway is associated with the development of cardiomyocyte apoptosis (El-Kashef et al. 2015; Gao et al. 2015; Li et al. 2015). The western blotting results showed that MI could remarkably suppress the expression levels of p-AKT, p-NF-κB, and TLR4, while SMCTHP could obviously increase p-AKT, p-NF-κB, and TLR4 protein expression, indicating that both the AKT and TLR4/NF-κB pathways may be the main pathways for anti-apoptotic mechanisms of SMCTHP in ischemic myocardium.

Given the above, a possible molecular mechanism of SMCTHP against ISO-triggered myocardial ischemic injury was presented (Fig. 11). SMCTHP treatment alleviated ISO-induced myocardial ischemic injury by regulating the alterations of apoptosis cascade reactions.

5. Conclusions

In conclusion, in the present study, network pharmacology determined 92 bioactive compounds and 246 relevant targets for MI in SMCTHP, forming an intricate compound-target network. The PPI network analysis identified twenty-five hub targets for SMCTCH treatment of MI. Further enrichment analysis revealed that the anti-MI targets were highly concerned with the apoptotic process, which might be one of principal pathway of SMCTHP against MI. In addition, an AMI rat model was used to access the anti-

apoptotic effects of SMCTHP. These findings suggested that SMCTHP exhibited the anti-apoptotic effects on ischemic rat myocardium, and the possible mechanism may be through activating the AKT pathway but suppressing the TLR4/NF-κB pathway.

Declarations

Ethics Approval

All procedures of the animal experiment were conducted according to National Guidelines for Experimental Animal Welfare at the Center for Animal Experiments and were approved by the Animal Ethics Committee of Shaanxi University of Chinese Medicine (Approval No.TCM-2019-030-E05).

Consent to participate

Not applicable

Consent to publish

Not applicable

Authors Contributions

DSB, BJQ, and WXP designed this study; WPF, GS, XZP, ZHH conducted the experiments; DSB, LN and LJ retrieved databases and analyzed data; DSB drafted the main manuscript text, while WXP and BJQ revised it. All authors read and approved the manuscript, and all data were generated in-house and that no paper mill was used.

Funding

This work was supported by the National Natural Science Foundation of China (CN) (No.81974544; No.81573624), the Project on Social Development of Shaanxi Provincial Science and Technology Department (No.2019SF-286), the Key Laboratory Project of Shaanxi Provincial Department of Education (No.18JS025).

Competing Interests

The authors declare that there are no conflicts of interest.

Availability of data and materials

The data used to support the findings of this study are included with the articles and available in the Supplementary Materials.

References

1. Al-Amran FF, Shahkolahi M (2014) Oxytocin ameliorates the immediate myocardial injury in rat heart transplant through downregulation of neutrophil-dependent myocardial apoptosis Transpl P 15(2):37–45. https://10.1016/j.transproceed.2013.03.022
2. Azad FM, Arabian M, Maleki M, Malakootian M (2020) Small molecules with big impacts on cardiovascular diseases Biochem Genet 58(3):359–383. https://doi.org/ 10.1007/s10528-020-09948-z.
3. Cao Y, Wang J, Su GZ et al (2016) Anti-myocardial ischemia effect of Syringa pinnatifolia Hemsl. by inhibiting expression of cyclooxygenase-1 and – 2 in myocardial tissues of mice J Ethnopharmacol 187(1):259–268. https://10.1016/j.jep.2016.04.039
4. Chen M, Wei YH, Hou YM et al (2021) Research progress on the animal models for heart failure J Med Theor Pract 34(7):1103–1105. https://10.19381/j.issn.1001-7585.2021.07.008.
5. Chen Y, Zhang N, Ma J et al (2016) A Platelet/CMC coupled with offline UPLC-QTOF-MS/MS for screening antiplatelet activity components from aqueous extract of Danshen J Pharmaceut Biomed 117(1):178–183. https://10.1016/j.jpba.2015.06.009
6. Chimenti MS, Sunzini F, Fiorucci L et al (2018) Potential role of cytochrome c and tryptase in psoriasis and psoriatic arthritis pathogenesis: Focus on resistance to apoptosis and oxidative stress Front Immunol 9:2363. https://10.3389/fimmu.2018.02363
7. Desagher S, Martinou JC (2000) Mitochondria as the central control point of apoptosis Trends Cell Biol 10(9):369–377. https://10.1016/S0962-8924(00)01803-1
8. Ding HS, Yang J, Chen P et al (2013) The HMGB1-TLR4 axis contributes to myocardial ischemia/reperfusion injury via regulation of cardiomyocyte apoptosis Gene 527(1):389–393. https://10.1016/j.gene.2013.05.041
9. El-Kashef DH, Serrya MS (2019) Sitagliptin ameliorates thioacetamide-induced acute liver injury via modulating TLR4/NF-KB signaling pathway in mice Life Sci 228:266–273. https://10.1016/j.lfs.2019.05.019
10. Fan YL, Hu LP, Zhu JH et al (2018) Experimental study on animal model of myocardial ischemia Lab Anim Sci 35(1):72–75. https://CNKI:SUN:SYDG.0.2018-01-014
11. Gao Y, Song G, Cao YJ et al (2019) The guizhi gancao decoction attenuates myocardial ischemia-reperfusion injury by suppressing inflammation and cardiomyocyte apoptosis Evid-based Compl Alt 2019:1947465. https://10.1155/2019/1947465
12. Hamacher-Brady A, Brady NR, Gottlieb RA (2006) The interplay between pro-death and pro-survival signaling pathways in myocardial ischemia/reperfusion injury: apoptosis meets autophagy Cardiovasc Drug Ther 20(1):445–462. https://10.1007/s10557-006-0583-7
13. Harris MH, Thompson CB (2000) The role of the Bcl-2 family in the regulation of outer mitochondrial membrane permeability Cell Death Differ 7(12):1182–1191. https://10.1038/sj.cdd.4400781
14. Hu GQ, Du X, Li YJ et al (2017) Inhibition of cerebral ischemia/reperfusion injury-induced apoptosis: nicotiflorin and JAK2/STAT3 pathway Neural Regen Res 12(1):96–102. https://10.4103/1673-5374.198992

15. Huang C, Zheng C, Li Y et al (2014) Systems pharmacology in drug discovery and therapeutic insight for herbal medicines Brief Bioinform 15(5):710–733. https://10.1093/bib/bbt035
16. Huang W, Yang Y, Zeng Z et al (2016) Effect of Salvia miltiorrhiza and ligustrazine injection on myocardial ischemia/reperfusion and hypoxia/reoxygenation injury Mol Med Rep 14(5):4537–4544. https://10.3892/mmr.2016.5822
17. Hori M, Nishida K (2009) Oxidative stress and left ventricular remodelling after myocardial infarction Cardiovasc Res 81(3):457–464. https://10.1093/cvr/cvn335
18. Jayachandran KS, Khan M, Selvendiran K et al (2010) Crataegus oxycantha extract attenuates apoptotic incidence in myocardial ischemia-reperfusion injury by regulating Akt and Hif-1 signaling pathways J Cardiovasc Pharmacol 56(5):526–531. https://10.1097/FJC.0b013e3181f64c51
19. Jian J, Xuan F, Qin F et al (2015) Bauhinia championii flavone inhibits apoptosis and autophagy via the PI3K/Akt pathway in myocardial ischemia/reperfusion injury in rats Drug Des Dev Ther 9(1):5933–5945. https://10.2147/DDDT.S92549
20. Kang M, Kim JH, Cho C, et al (2007) Anti-ischemic effect of *Aurantii Fructus* on contractile dysfunction of ischemic and reperfused rat heart J Ethnopharmacol 111(3):584–591. https://10.1016/j.jep.2007.01.007
21. Kang YJ (2008) Herbogenomics: from traditional Chinese medicine to novel therapeutics Exp Biol Med 233(9):1059–1065. https://10.3181/0802-MR-47
22. Li F, Duan J, Zhao M et al (2019) A network pharmacology approach to reveal the protective mechanism of *Salvia miltiorrhiza-Dalbergia odorifera* coupled-herbs on coronary heart disease Sci Rep 9:19343. https://10.1038/s41598-019-56050-5
23. Li H, Yang H, Wang D et al (2020) Peroxiredoxin2 (Prdx2) reduces oxidative stress and apoptosis of myocardial cells induced by acute myocardial infarction by inhibiting the TLR4/Nuclear factor kappa B (NF-kappaB) signaling pathway Med Sci Monitor 26:e926281. https://10.12659/MSM.926281
24. Li J, Cao GY, Zhang XF et al (2020) Chinese medicine She-Xiang-Xin-Tong-Ning, containing moschus, corydalis and ginseng, protects from myocardial ischemia injury via angiogenesis Am J Chinese Med 48(1):107–126. https://10.1142/S0192415X20500068
25. Lin R, Duan J, Mu F et al (2018) Cardioprotective effects and underlying mechanism of *Radix Salvia Miltiorrhiza* and *Lignum Dalbergia Odorifera* in a pig chronic myocardial ischemia model Inter J Mol Med 42(5):2628–2640. https://10.3892/ijmm.2018.3844
26. Liu YT, Jia HM, Chang X, et al (2014) Tabolic pathways involved in Xin-Ke-Shu protecting against myocardial infarction in rats using ultra high-performance liquid chromatography coupled with quadrupole time-of-flight mass spectrometry," J Pharmaceut Biomed 90(1):35–44, 2014. https://10.1016/j.jpba.2013.11.008
27. Lu XH, Zhang L, Wen JX et al (2018) Research progress of rat model of heart failure Evaluation Anal Drug-Use Hosp China 18(11):1444–1446 + 1449. https://10.14009/j.issn.1672-2124.2018.11.002
28. Luan Y, Sun C, Wang J et al (2019) Baicalin attenuates myocardial ischemia-reperfusion injury through Akt/NF-kappaB pathway J Cell Biochem 120(3):3212–3219. https://10.1002/jcb.27587

29. Luo TT, Lu Y, Yan SK et al (2020) Network pharmacology in research of chinese medicine formula: methodology, application and prospective Chin J Intergr Med 26(1):72–80. https://10.1007/s11655-019-3064-0
30. Lyu M, Yan CL, Liu HX et al (2017) Network pharmacology exploration reveals endothelial inflammation as a common mechanism for stroke and coronary artery disease treatment of Danhong injection Sci Rep 7:15427. https://10.1038/s41598-017-14692-3
31. Ma C, Jiang Y, Zhang X et al (2018) Isoquercetin ameliorates myocardial infarction through anti-inflammation and anti-apoptosis factor and regulating TLR4-NF-kappaB signal pathway Mol Med Rep 17(5):6675–6680. https://10.3892/mmr.2018.8709
32. Martini M, De SMC, Braccini L et al (2014) PI3K/AKT signaling pathway and cancer: an updated review Ann Med 46(6):372–383. https://10.3109/07853890.2014.912836
33. Misao J, Hayakawa Y, Ohno M et al (1996) Expression of bcl-2 protein, an inhibitor of apoptosis, and Bax, an accelerator of apoptosis, in ventricular myocytes of human hearts with myocardial infarction Circulation 94(7):1506–1512. https://10.1161/01.CIR.94.7.1506
34. Nederhoff MGJ, Fransen DE, Verlinde S et al (2019) Effect of vagus nerve stimulation on tissue damage and function loss in a mouse myocardial ischemia-reperfusion model Auton Neurosci-Basic 221:102580. https://10.1016/j.autneu.2019.102580
35. Negoro S, Oh H, Tone E et al (2001) Glycoprotein 130 regulates cardiac myocyte survival in doxorubicin-induced apoptosis through phosphatidylinositol 3-kinase/Akt phosphorylation and Bcl-xL/caspase-3 interaction Circulation 103(4):555–561. https://10.1161/01.CIR.103.4.555
36. Orgah JO, He S, Wang YL, et al (2020) Pharmacological potential of the combination of *Salvia miltiorrhiza* (Danshen) and *Carthamus tinctorius* (Honghua) for diabetes mellitus and its cardiovascular complications Pharmacol Res 153:104654. https://10.1016/j.phrs.2020.104654
37. Ou L, Lin S, Song B et al (2017) The mechanisms of graphene-based materials-induced programmed cell death: a review of apoptosis, autophagy, and programmed necrosis Int J Nanomed 12(1):6633–6646. https://10.2147/IJN.S140526
38. Qu K, Cha H, Ru Y et al (2021) Buxuhuayu decoction accelerates angiogenesis by activating the PI3K-Akt-eNOS signalling pathway in a streptozotocin-induced diabetic ulcer rat model J Ethnopharmacol 273:113824. https://10.1016/J.JEP.2021.113824
39. Qu C, Xu DQ, Yue SJ et al (2020) Pharmacodynamics and pharmacokinetics of Danshen in isoproterenol-induced acute myocardial ischemic injury combined with Honghua J Ethnopharmacol 247:112284. https://10.1016/j.jep.2019.112284
40. Sanches-Silva A, Testai L, Nabavi SF et al (2020) Therapeutic potential of polyphenols in cardiovascular diseases: Regulation of mTOR signaling pathway Pharmacol Res 152:104626. https://10.1016/j.phrs.2019.104626
41. Shen J, Yang K, Sun C et al Analysis of active components in Salvia miltiorrhiza injection based on vascular endothelial cell protection Acta Pharmaceut 64(3):325–334. https://10.2478/acph-2014-0027

42. Shirai K (2004) Obesity as the core of the metabolic syndrome and the management of coronary heart disease Curr Med Res Opin (3):295–304. https://10.1185/030079903125003008
43. Song YF, Zhao L, Wang BC et al (2020) The circular RNA TLK1 exacerbates myocardial ischemia/reperfusion injury via targeting miR-214/RIPK1 through TNF signaling pathway Free Radical Bio Med 155(1):69–80. https://10.1016/j.freeradbiomed.2020.05.013
44. Teringova E, Tousek P (2017) Apoptosis in ischemic heart disease J Transl Med 15:87. https://10.1186/s12967-017-1191-y
45. Tian YF, Li LY, Wang R et al (2005) Compound danshen dropping pills: an overview of its protective effect on heart Acta Chin Med and Pharmacol 33(3):60–61. https://10.19664/j.cnki.1002-2392.2005.06.036
46. Uchiyama T, Engelman RM, Maulik N, Das DK (2004) Role of Akt signaling in mitochondrial survival pathway triggered by hypoxic preconditioning Circulation 109(24):3042–3049. https://10.1161/01.CIR.0000130647.29030.90
47. Wang N, Liu W, Zhou Y et al (2019) In vitro activities of nemonoxacin and other antimicrobial agents against human mycoplasma and ureaplasmas isolates and their defined resistance mechanisms Front Microbiol 10:1890. https://10.3389/fmicb.2019.01890
48. Wang XP, Wang PF, Bai JQ et al (2019) Investigating the effects and possible mechanisms of danshen-honghua herb pair on acute myocardial ischemia induced by isoproterenol in rats Biomed Pharmacother 40(12):1711–1716. https://10.1016/j.biopha.2019.109268
49. Wang XP, Wang PF, Bai JQ et al (2017) Comparative study on effect of *Salvia miltiorrhiza* and *Carthamus tinctorius* compatibility on activity of drug-metabolism enzymes in male and female rats with myocardial ischemia Drug Evaluation Res 40(21):1711–1716. https://10.7501/j.issn.1674-6376.2017.12.007
50. Wang YL, Zhang Q, Yin SJ et al (2019) Screening of blood-activating active components from Danshen-Honghua herbal pair by spectrum-effect relationship analysis Phytomedicine 54(1):149–158. https://10.1016/j.phymed.2018.09.176
51. Xu MC, Shi HM, Gao XF et al (2013) Salidroside attenuates myocardial ischemia-reperfusion injury via PI3K/Akt signaling pathway J Asian Nat Prod Res 15(3):244–252. https://10.1080/10286020.2012.762358
52. Yue SJ, Xin LT, Fan YC et al (2017) Herb pair Danggui-Honghua: mechanisms underlying blood stasis syndrome by system pharmacology approach Sci Rep 7:40318. https://10.1038/srep40318
53. Yue Y, Yang X, Feng KN et al (2017) M2b macrophages reduce early reperfusion injury after myocardial ischemia in mice: A predominant role of inhibiting apoptosis via A20 Int J Cardiol 245(1):228–235. https://10.1016/j.ijcard.2017.07.085
54. Zhao ZQ, Velez DA, Wang NP et al (2001) Progressively developed myocardial apoptotic cell death during late phase of reperfusion Apoptosis 6(4):279–290. https://10.1023/A:1011335525219
55. Zhu JZ, Bao XY, Zheng Q et al (2019) Buyang huanwu decoction exerts cardioprotective effects through targeting angiogenesis via caveolin-1/VEGF signaling pathway in mice with acute

Figures

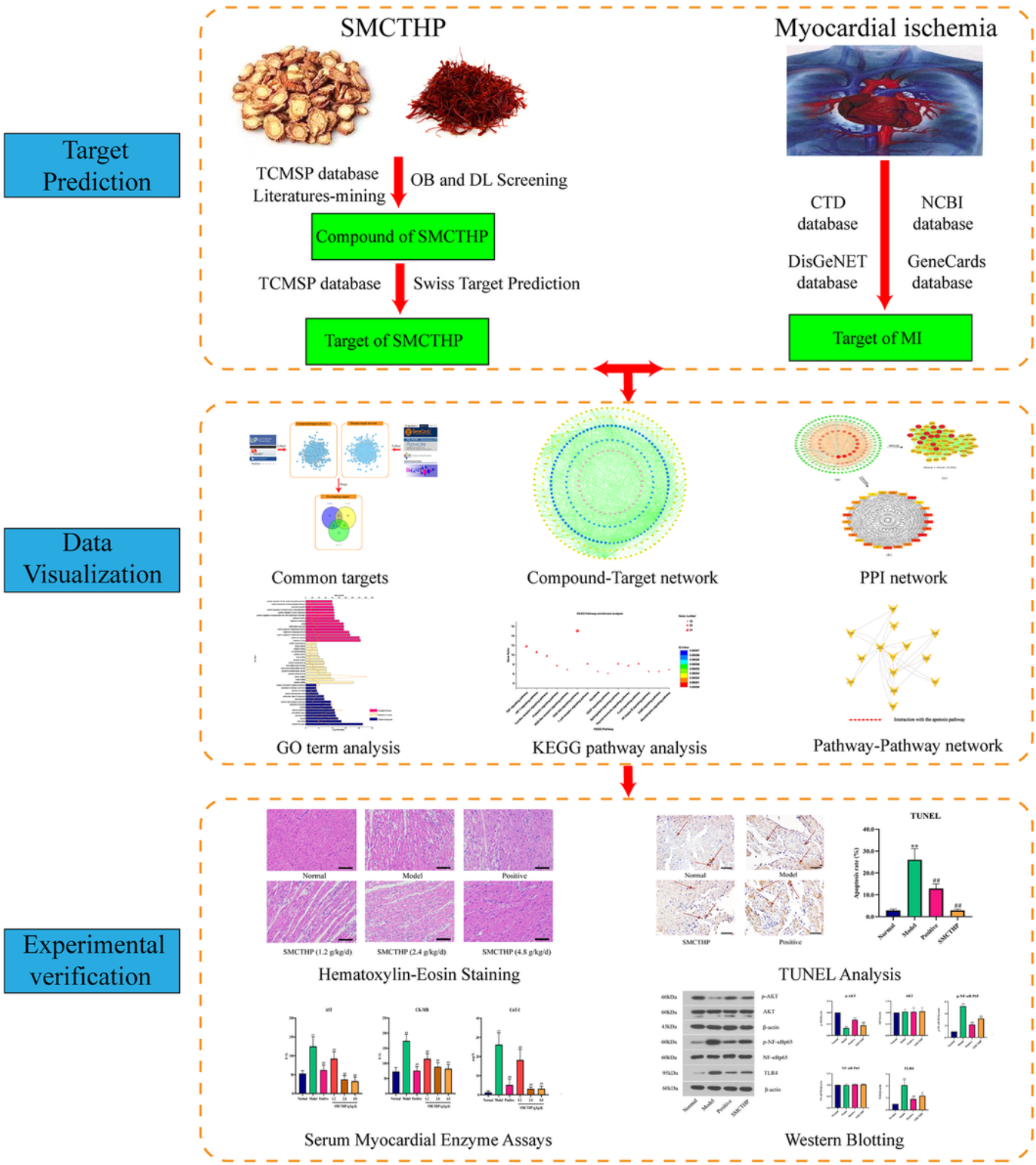

Figure 1

The flowchart reveals the protective mechanism of SMCTHP in the treatment of MI.

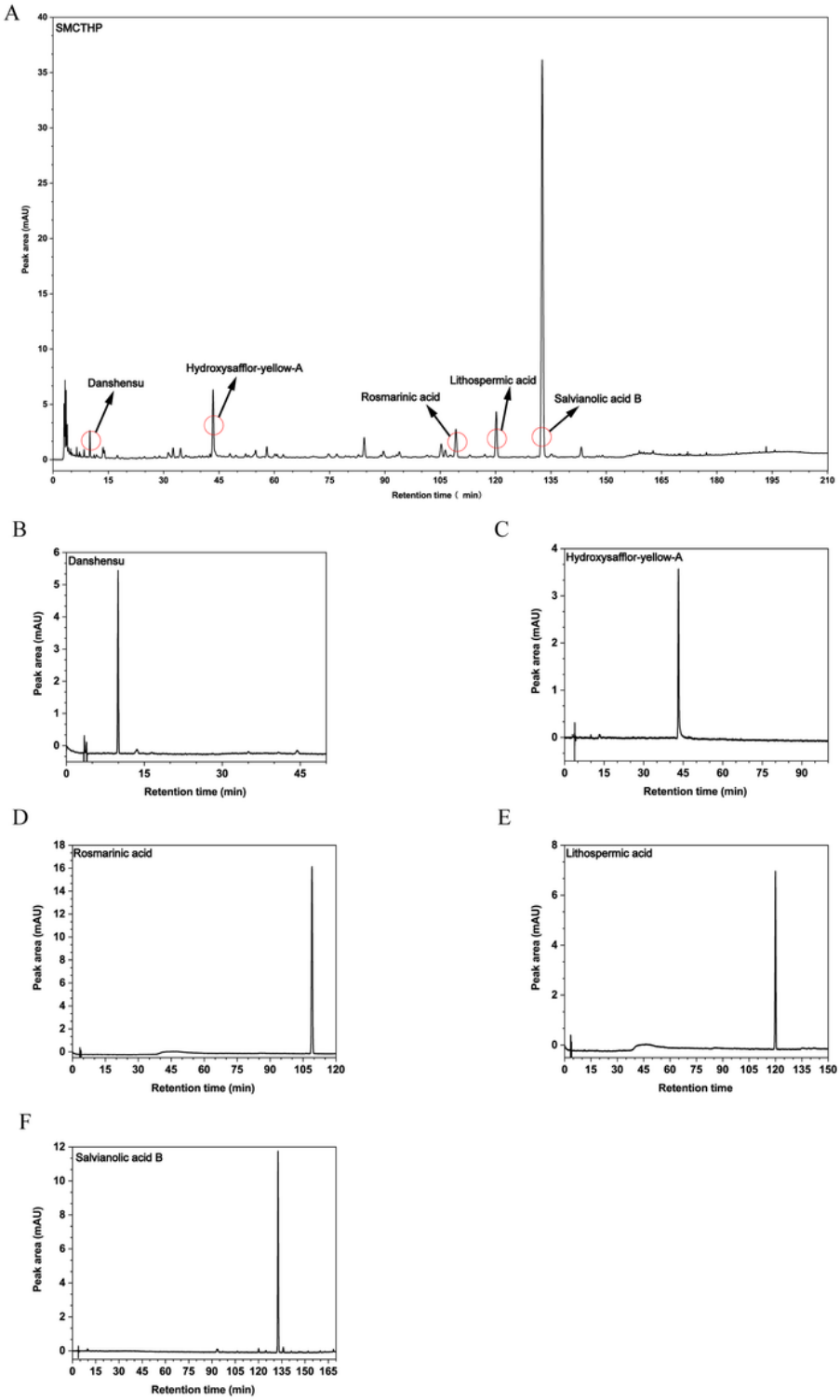

Figure 2

Quality control of SMCTHP sample. **A** The HPLC chromatograms of SMCTHP sample. **B-F** The HPLC chromatograms of five standards.

Figure 3

Candidate target screening of the SMCTHP for myocardial ischemia treatment.

Figure 4

Compounds-Targets' visual network. The dark blue squares represent the compounds of SM, dark blue triangles represent the compounds of CT, dark blue regular octagons represent overlapping compounds of SM and CT, pink circles represent targets acted on alone by CT, light blue circles represent targets acted alone by SM, yellow circles indicate SM-CT intersection proteins.

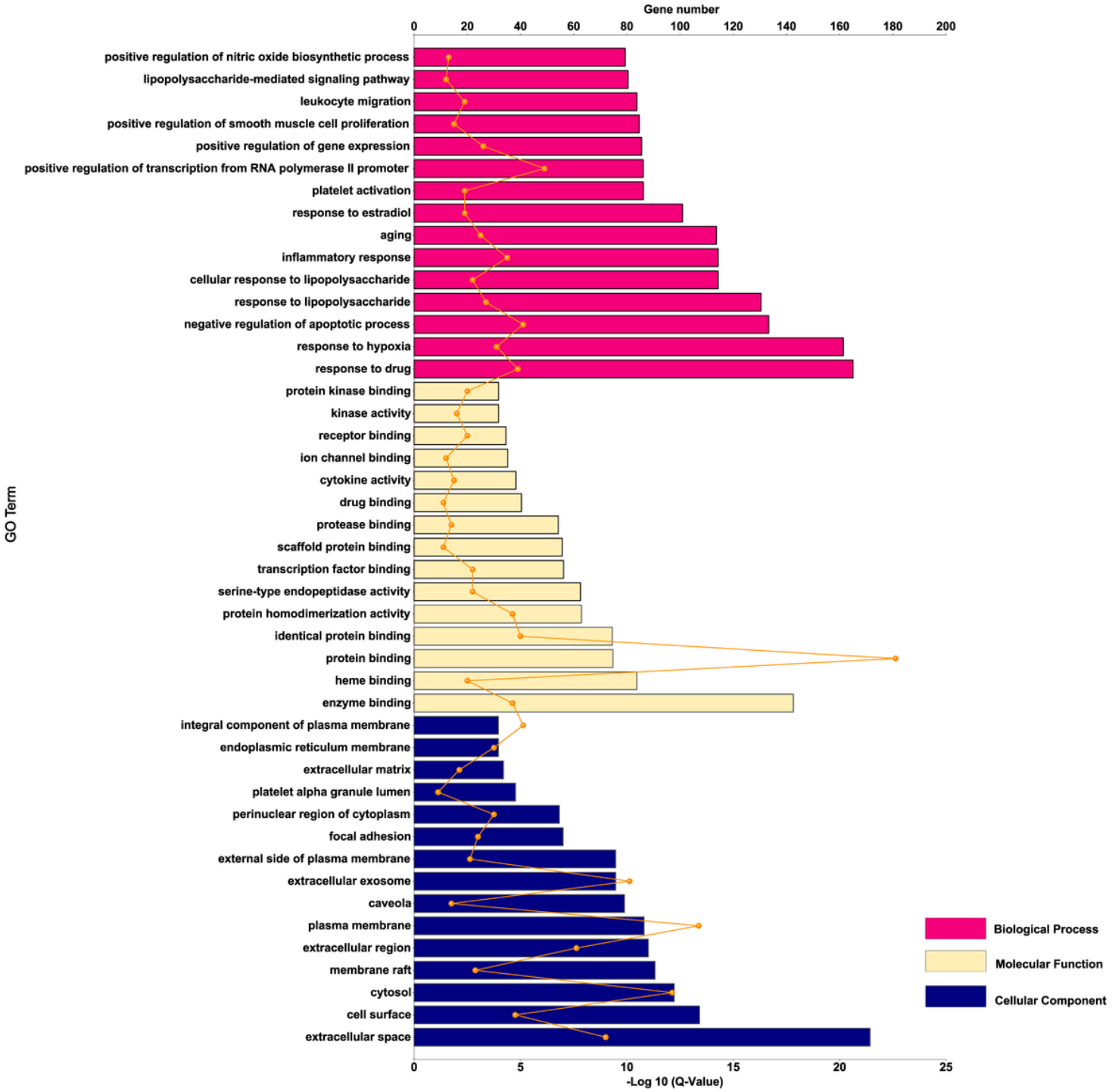

Figure 5

GO enrichment analysis for anti-MI targets of SMCTHP. The order of importance was ranked from bottom to top by −Log10 (Q-Value) with bar chart. The number of targets stick into each term with line chart.

Figure 6

KEGG enrichment analysis of anti-MI targets of SMCTHP. **A** Top 15 significant KEGG pathways which related to myocardial ischemia for targets of SMCTHP. The bubble size represents the number of the target in the enriched pathway terms, bubble color represents the pathway's q-value. **B** Pathway-Pathway interaction network. Different nodes represent different pathways, these pathways interact with each other and form a pathway network. The apoptosis pathway interacts with multiple pathways.

Figure 7

The protein–protein interaction (PPI) networks analysis. **A** PPI network of targets of SMCTHP in treating of myocardial ischemia. **B** Twenty-five hub targets were identified from the PPI network by the Cytohubba analysis, the color of a node changes from yellow to red indicating that the node is becoming more important. **C** The top 1 module was screened from the PPI network by the MCODE analysis, and the module score is 23.895. The apoptosis-related targets in the module were marked in red.

Figure 8

The effects of SMCTHP on histology and myocardial specific enzymes in serum. (a) The histopathologic changes of the heart sections of rat between different groups in HE staining (magnification × 200, scale bars, 10 μM). (b) Serum levels of AST, CK-MB, and CTn-I. Data were represented as mean ± SD (n = 8), $^{*}P < 0.05$, $^{**}P < 0.01$ versus normal group. $^{\#}P < 0.05$, $^{\#\#}P < 0.01$versus model group.

Figure 9

Effect of the SMCTHP on the cardiomyocyte apoptosis in ischemic rat myocardium. **A** TUNEL staining for the evaluation of cardiomyocyte apoptosis. The TUNEL positive cardiomyocytes nuclei were stained with brownish yellow and indicated with red arrows. The right shows percentage of positive apoptosis cardiomyocyte (magnification × 200, scale bars, 10 μM) (n = 6). **B** Protein expression of Cytochrome c, Caspase 8, Caspase-7, Caspase-9, Caspase-3, Bax, and Bcl-2 in rat myocardial tissues. GAPDH was used

as control. Data were represented as mean ± SD (n = 3), $^{*}P < 0.05$, $^{**}P < 0.01$ versus normal group. $^{\#}P < 0.05$, $^{\#\#}P < 0.01$versus model group.

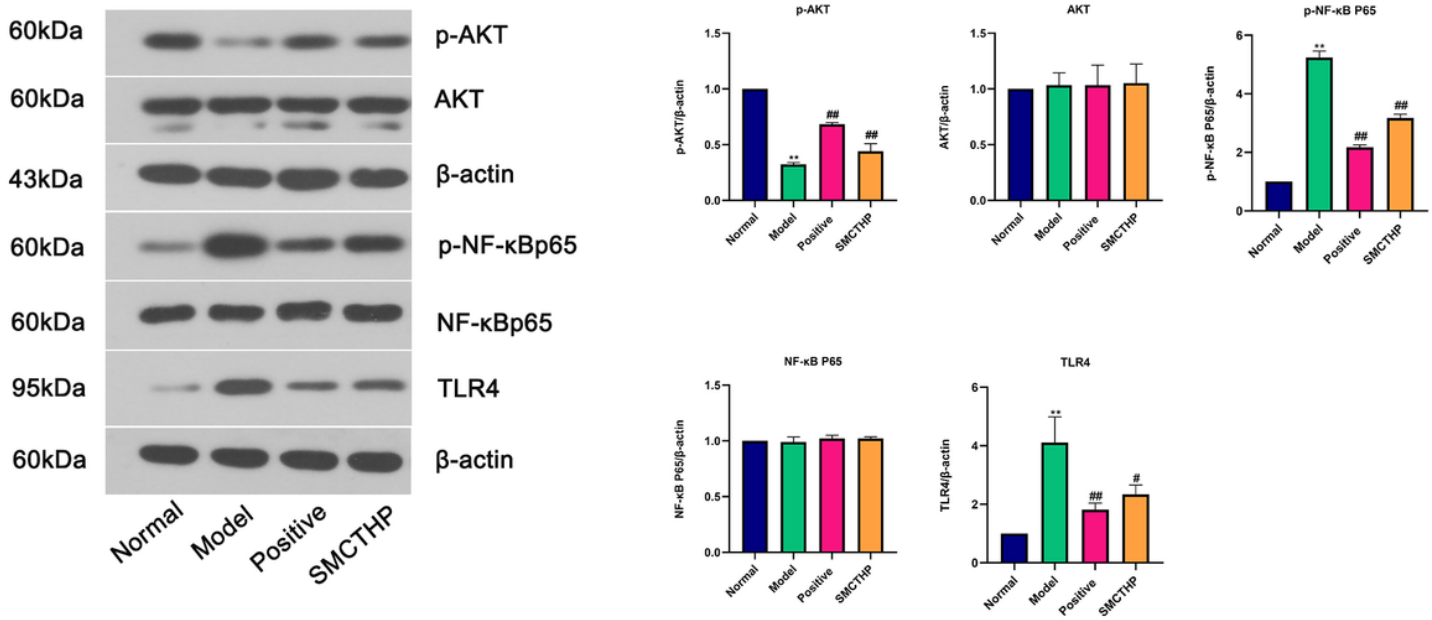

Figure 10

Effect of the SMCTHP on the expression levels of p-AKT, AKT, p-NF-κBp65, p-NF-κBp65, and TLR4 in rat myocardial tissues. β-actin was used as control. Data were represented as mean ± SD (n = 3), $^{*}P < 0.05$, $^{**}P < 0.01$ versus normal group. $^{\#}P < 0.05$, $^{\#\#}P < 0.01$versus model group.

Figure 11

The possible action diagram of SMCTHP against ISO-induced myocardial ischemic injury. SMCTHP regulated the protein expressions of targets associated with apoptosis in response to overdose ISO challenge in rat.

Supplementary Files

This is a list of supplementary files associated with this preprint. Click to download.

- SupplementaryTable1.xlsx

- SupplementaryTable2.xlsx
- SupplementaryTable3.xlsx
- SupplementaryTable4.xlsx
- SupplementaryTable5.xlsx
- SupplementaryTable6.xlsx
- SupplementaryTable7.xlsx
- SupplementaryTable8.xlsx